Sonar Pulse Detection Using Chirp Rate Estimation and CFAR Algorithms

Karol ABRATKIEWICZ

Gdansk University of Technology, Faculty of Electronics, Telecommunications and Informatics
G.Narutowicza 11/12, 80-980 Gdansk, Poland, Email: karol.abratkiewicz@gmail.com

This paper presents a new approach to sonar pulse detection. The method uses chirp rate estimators and algorithms for the adaptive threshold, commonly used in radiolocation. The proposed approach allows detection of pulses of unknown parameters, which may be used in passive hydrolocation or jamming detection in underwater communication. Such an analysis is possible thanks to a new kind of imaging, which presents signal energy in the function of chirp rate. The proposed method relies on chirp rate estimation of the received signal, and the calculation of the local threshold level depends on noise and reverberations which make detection of a particular type of signal possible.

Keywords: electronic warfare, signal features, signal detection.

1. Introduction

Detection of sonar pulses is a technique widely described in the literature [1–4]. This is a very important task in the field of combat, and in electronic warfare in the aquatic environment. The problem is to choose a detection threshold value that is strongly dependent on the propagation conditions, the presence of other devices, and the parameters of the system being used. Too high a detection threshold in a variable environment can result in no signal being detected, while too low a threshold will cause the noise to exceed it. The proposed method is free of this problem. It not only detects the existence of a transmitter, but also allows the identification and classification of these signals.

Part 2 shows the theoretical basics for chirp rate estimation. Used approach and the mathematical foundations are described. Part 3 describes three CFAR algorithms used in this method to calculate the adaptive detection threshold. Part 4 contains simulation results for three estimators and three CFAR algorithms.

2. Chirp rate estimation

There are several methods of chirp rate estimation [5–7]. The selected method uses the approach described in [7] and according to this, the process is based on operations on a short-time

Fourier transform. By modifying the signal in the time-frequency domain, it is possible to distinguish information about the phase changes of each components. The following terminology will be useful for describing estimators. $x(t)$ is a time domain signal defined as:

$$x(t) = A_x(t)\exp(j\Phi_x(t)), \tag{1}$$

characterized by the amplitude and phase described respectively:

$$A_x(t) = \mathcal{A}_x\exp(-(t - t_x)^2/(2T_x^2)), \tag{2}$$

$$\Phi_x(t) = \phi_x + \omega_x t + \alpha t^2/2, \tag{3}$$

where ω_x is pulsation, α is chirp rate. Then, the short-time Fourier transform on signal $x(t)$ can be calculated using following manner:

$$F_x^h(t,\omega) = \int_{\mathbb{R}} x(u)h(t-u)e^{-j\omega u}\mathrm{d}u = e^{-j\omega u}\int_{\mathbb{R}} x(t-u)h(u)e^{j\omega u}\mathrm{d}u. \tag{4}$$

In Eq. (4) the window $h(t)$ is used, but in general it is possible to use the window derivative (n-th order) as well as window multiplied by time ramp (also n-th order), respectively:

$$\mathcal{D}^n h(t) = \frac{d^n h(t)}{dt^n}, \tag{5}$$

$$\mathcal{T}^n h(t) = t^n h(t). \tag{6}$$

In STFT symbol $F_x^h(t,\omega)$, lower index indicates signal under consideration, and higher index corresponds to used window. According to the above terminology, it is possible to introduce three chirp rate estimators respectively $\mathfrak{K}$, $\mathfrak{D}$, $\mathfrak{F}$.

$$\mathfrak{K}(t,\omega) = \frac{\Re(F_x^{\mathcal{D}h}(t,\omega)F_x^h(t,\omega)^*)}{\Im(F_x^{\mathcal{T}h}(t,\omega)F_x^h(t,\omega)^*)}, \tag{7}$$

$$\mathfrak{D}(t,\omega) = \Im\left(\frac{F_x^{\mathcal{D}^2 h}(t,\omega)F_x^h(t,\omega) - F_x^{\mathcal{D}h}(t,\omega)^2}{F_x^{\mathcal{D}h}(t,\omega)F_x^{\mathcal{T}h}(t,\omega) - F_x^{\mathcal{T}\mathcal{D}h}(t,\omega)F_x^h(t,\omega)}\right), \tag{8}$$

$$\mathfrak{F}(t,\omega) = \Im\left(\frac{F_x^{\mathcal{T}\mathcal{D}h}(t,\omega)F_x^h(t,\omega) + F_x^h(t,\omega)^2 - F_x^{\mathcal{T}h}(t,\omega)F_x^{\mathcal{D}h}(t,\omega)}{F_x^{\mathcal{T}h}(t,\omega)^2 - F_x^{\mathcal{T}^2 h}(t,\omega)F_x^h(t,\omega)}\right), \tag{9}$$

where $(\cdot)^*$ is the complex conjugate, $\Re$ is real part, as well as $\Im$ is imaginary part. The $\mathfrak{K}$ estimator is based on the first derivative of the window $h(t)$. The $\mathfrak{D}$ estimator is generated by differentiation $\mathfrak{K}$ estimator with respect to time (separately numerator and denominator), and the $\mathfrak{F}$ estimator is generated by differentiation of the $\mathfrak{K}$ estimator with respect to frequency (also separately the numerator and the denominator).

Fig. 1 presents chirp rate estimation results for simulated signal with chirp rate $\alpha = 500Hz/s$, sampled with frequency $f_s = 1000$Hz with SNR=20dB. All images were obtained by using [8]. Fig. 1a presents accelerogram in time-frequency domain, and Fig. 1b shows an example $\mathcal{R}$ profile. The second image is similar to the histogram, because it checks the amount of each chirp rate values of a given range. Profile additionally contains information about the energy carried by a particular component, characterized by a given chirp rate.
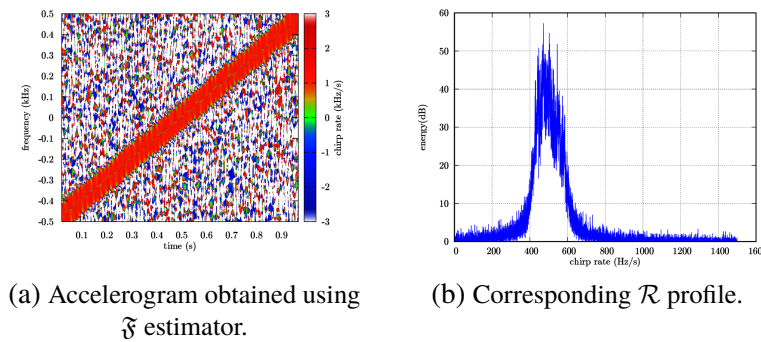
(a) Accelerogram obtained using $\mathfrak{F}$ estimator.

(b) Corresponding $\mathcal{R}$ profile.

Fig. 1. Chirp rate estimation results. Accelerogram (a) and $\mathcal{R}$ profile (b).

3. Constant False Alarm Rate Algorithms

CFAR algorithms are commonly known in radiolocation and hydrolocation [9–16]. In general, these are algorithms that allow one to estimate the adaptive threshold depending on noise and interference. The conventional approach assumes the analysis of the received signal's spectrum and the detection of peaks with energy exceeding the noise level. In a variable propagation environment, the detection threshold must be reconfigurable, which can be achieved by these algorithms. Fig. 2 shows a simplified block diagram of this method. The structure performs calculations for each point of the data vector. In a single iteration, the CUT (Cell Under Test) is processed. Around it there are M guard cells ($M/2$ on each side of CUT), ignored during calculation (in blue). Reference cells are colored in green. The number of these cells is determined and is N ($N/2$ on each side of CUT). The reference cells are summed (independently, on each side of the CUT) and fed to a logic block whose functionality depends on the selected algorithm. The result of the calculation is multiplied by the scaling factor and then passed to the detector where it is decided whether the object was detected or not.
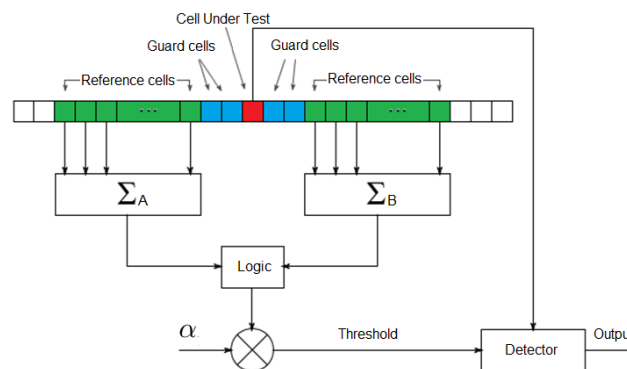

Fig. 2. CFAR block diagram.

In general, the detection threshold is calculated as the product of the scaling factor and the noise power estimates according to the following expression:

$$T = \alpha \cdot P_n, \tag{10}$$

where α is the scaling factor (depends on selected algorithm), and P_n is the power noise estimate. This article presents 3 selected algorithms. The first one is CA CFAR (Cell Averaging Constant

False Alarm Rate). The detection threshold for this method is determined as follows:

$$T_{\text{CA}} = N(P_{\text{fa}}^{-1/N} - 1) \cdot \frac{1}{N} \sum AB, \tag{11}$$

where N is is the number of reference cells, P_{fa} is the probability of a false alarm, while the sum $\sum AB$ is, according to Fig. 2, the summed reference cell values on both sides of the CUT. The first component of the product $\alpha = N(P_{\text{fa}}^{-1/N} - 1)$ is a scaling factor and the second is the noise power estimate $P_n = \frac{1}{N} \sum AB$. The same approach applies to the other two algorithms. The second one is GOCA CFAR (Greatest of Cell Averaging CFAR). This is a modification of the first discussed method, and assumes noise power estimates as the greatest of the $\sum A$ and $\sum B$. The expression is described as follows:

$$T_{\text{GOCA}} = N(P_{\text{fa}}^{-1/N} - 1) \cdot \max\left(\sum A, \sum B\right). \tag{12}$$

The symbols are the same as in the CA CFAR method. The last considered approach is OS CFAR (Order Statistic CFAR). The method uses the percentile calculated from the $\sum A$ and $\sum B$ as the noise power estimate. In this approach, the scaling factor is calculated differently from the two methods discussed. In general, the detection threshold is calculated as follows:

$$T_{\text{OS}} = \ln\left(\frac{1}{P_{\text{fa}}}\right) \cdot \text{percentile}\left(\sum A, \sum B\right). \tag{13}$$

A block that realizes the described CFAR algorithms can be located directly after the signal amplifier at the receiver, or at the output of the matched filter. In the first case, however, it is required that the SNR level is no less than 0dB (which in most cases is unreachable).
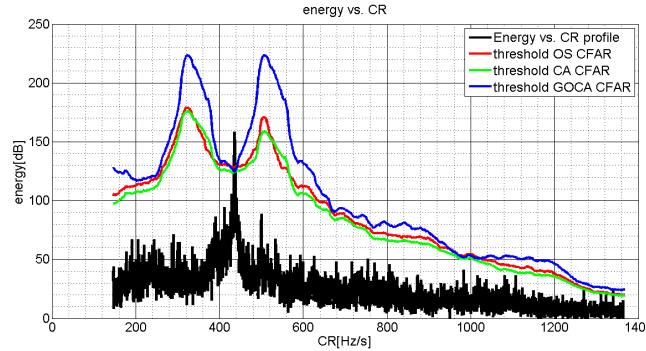

Fig. 3. Example of sonar pulse detection.

Fig. 3 shows an example of the results of sonar pulse detection. The simulated received signal was represented in the time-frequency domain, the chirp rate of pulse was calculated, and the results were presented as an $\mathcal{R}$ profile. This profile was used as the input vector for the CFAR algorithms. The figure shows how the detection threshold changes its local value depending on the level of noise on the $\mathcal{R}$ profile.

4. Results

As part of the experiment, the minimum likelihood of a false alarm with which the system can work is investigated. This is information about the reliability of the whole device. The test

Tab. 1. Signal parameters.

Chirp rate $\frac{Hz}{s}$	Carrier freuency [kHz]	Pulse duration [ms]	Sampling rate [kHz]	SNR[dB]
750	1	10	3	0,10,20,30,40

Tab. 2. CFAR algorithms parameters.

Number of points on $\mathcal{R}$ profile	N	M	Percentile (OS CFAR) %
4096	200	100	60

signal input was a sample sonar pulse with the parameters given in Tab. 1, and Tab. 2 presents CFAR algorithms assumptions. For each SNR of $\{0, 10, 20, 30, 40\}$ and for each estimator ($\mathfrak{K}$, $\mathfrak{D}$ and $\mathfrak{F}$), the minimum probability of a false alarm was calculated. The results are shown in Fig. 4.
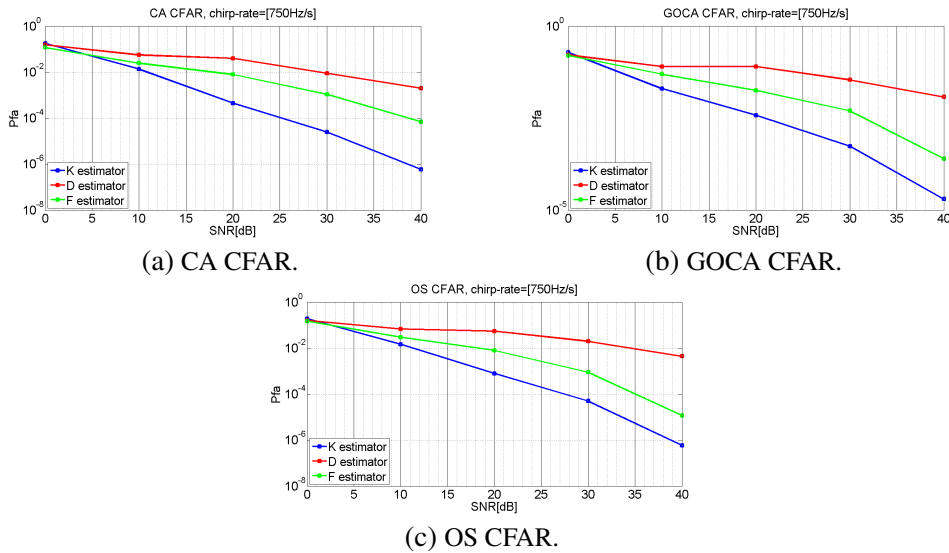

(a) CA CFAR.

(b) GOCA CFAR.

(c) OS CFAR.

Fig. 4. Minimum probability of false alarm for all SNR and chirp rate values and each CFAR algorithm.

It turns out that, contrary to expectations, the best results for each algorithm are the estimator $\mathfrak{K}$ (the system can work with the lowest probability of false alarm). Theoretically, this estimator is characterized by the worst parameters: it is ineffective for AM modulation signals, and near the attractor (the line around which the energy of component in the time-frequency domain is focused) the accuracy of the estimator is near to zero. For the selected chirp rate representation method, components for which the accuracy of the estimation is close to zero are outside the profile area $\mathcal{R}$. Due to the limited range of observation of the chirp rate, the estimation errors for the estimator $\mathfrak{K}$ are omitted. It should also be noted that the results are correct for the given simulation conditions and the assumed time window width (83ms). Estimator $\mathfrak{F}$ was worse than estimator $\mathfrak{K}$, while for estimator $\mathfrak{D}$ the worst results were obtained. The charts for the CFAR algorithms are similar, and the convergence of the results is perceptible.

5. Conclusion

In this paper a new approach to sonar pulse detection has been examined. The basic concept of chirp rate estimation has been introduced, and three CFAR algorithms have been selected and implemented to adapt the selection of detection thresholds in the presence of noise.

The paper compares the results of the sonar pulses detection for the three introduced chirp rate estimators and the three discussed CFAR algorithms.

References

[1] J. Liang, K.M. Wong, Detection of Narrow-Band Sonar Signal on a Riemannian Manifold, 2015 IEEE 28th Canadian Conference on Electrical and Computer Engineering (CCECE), pp. 959-964.

[2] R.W. Mill, G.J. Brown, Auditory-inspired Interval Statistic Receivers for Passive Sonar Signal Detection, OCEANS 2007 - Europe, pp. 1-6.

[3] K. Ugrinovic, O. Ponic, An outline of the passive sonar signal detection, Proceedings. Elmar-2004. 46th International Symposium on Electronics in Marine, pp. 247-251.

[4] M.K. Ward, M. Stevenson, Sonar Signal Detection and Classification using Artificial Neural Networks, 2000 Canadian Conference on Electrical and Computer Engineering, vol. 2 pp. 717-721.

[5] K. Czarnecki, The instantaneous frequency rate spectrogram, Mechanical Systems and Signal Processing, vol.66-67, pp. 361-373, 2016.

[6] A.E. Barnes, The calculation of instantaneous frequency and instantaneous bandwidth, Geophysics, vol. 57, no. 11, pp. 1520-1524. 1992.

[7] D. Fourer, F. Auger, K. Czarnecki, S. Meignen, P. Flandrin, Chirp rate and instantaneous frequency estimation: application to recursive vertical synchrosqueezing, IEEE Signal Processing Letters, vol. 24, no. 11, pp. 1724-1728, 2017.

[8] F. Auger, K. Czarnecki, D. Fourer, ccROJ - Time-Frequency C++ Framework, SoftwareX, 2017. Project webpage: https://github.com/dsp-box/ccROJ.

[9] L. Anitori, M. Otten, A. Maleki, Compressive CFAR Radar Detection, 2012 IEEE Radar Conference, pp. 320-325.

[10] P.P. Gandhi, S.A. Kassam, Analysis of CFAR Processors in Nonhomogeneous Background, IEEE Transactions On Aerospace And Electronic Systems, vol. 24, no. 4, 1988.

[11] M. Barkat, S. Dib, CFAR detection for two correlated targets, Signal Processing, vol. 61, no. 3, pp. 289-295, 1997.

[12] Y. Sun, M. Farooq, T.K. Robb, Adaptive CFAR active sonar signal thresholding using radial basis functional neural networks, Proceedings of the 36th IEEE Conference on Decision and Control, vol. 3, pp. 2193-2198, 1997.

[13] B. Kalyan, A. Balasuriya, Sonar based automatic target detection scheme for underwater environments using CFAR techniques: a comparative study, Proceedings of the 2004 International Symposium on Underwater Technology, pp. 33-37.

[14] V. Anastassopoulos, G. Lampropoulos, A New and Robust CFAR Detection Algorithm, IEEE Transactions on Aerospace and Electronic Systems, vol. 28, no. 2, pp. 420-427, 1992

[15] H. Dai, L Du, Y. Wang, A Modified CFAR Algorithm Based on Object Proposals for Ship Target Detection in SAR Images, IEEE Geoscience and Remote Sensing Letters vol. 13, no. 12, pp. 1925-1929, 2016.

[16] G.G. Acosta, S.A. Villar, Accumulated CA-CFAR Process in 2-D for Online Object Detection From Sidescan Sonar Data, IEEE Journal of Oceanic Engineering vol. 40, no. 3, pp. 558-569, 2015.